Colloid Polym Sci (2017) 295:1305–1312
DOI 10.1007/s00396-017-4044-6

INVITED ARTICLE

Thermo-induced multistep assembly of double-hydrophilic block copolypeptoids in water

Anna Bogomolova[1] · **Christian Secker**[1] · **Joachim Koetz**[2] · **Helmut Schlaad**[2]

Received: 12 January 2017 / Revised: 27 January 2017 / Accepted: 8 February 2017 / Published online: 6 March 2017

Abstract The aqueous solution behavior of thermoresponsive-hydrophilic block copolypeptoids, i.e., poly(*N*-(*n*-propyl)glycine)$_x$-*block*-poly(*N*-methylglycine)$_y$ (x = 70; y = 23, 42, 76), in the temperature range of 20–45 °C is studied. Turbidimetric analyses of the 0.1 wt% aqueous solutions reveal two cloud points at T_{cp}~30 and 45 °C and a clearing point in between at T_{cl}~42 °C. Temperature-dependent dynamic light scattering (DLS) suggest that right above the first collapse temperature, single polymer molecules assemble into large structures which upon further heating, i.e., at the clearing point temperature, disassemble into micelle-like structures. Upon further heating, the aggregates start to grow again in size, as recognized by the second cloud point, through a crystallization process.

Keywords Polypeptoids · Block copolymers · Thermoresponsive · Self-assembly

Introduction

Polypeptoids, i.e., poly(*N*-alkyl glycine)s, are an emerging class of bioinspired materials mimicking polypeptides [1]. The physico-chemical properties of polypeptoids and the aggregation/self-assembly behavior can be tuned by variation of the *N*-alkyl side chains. Polypeptoids with short alkyl chains, up to three carbon atoms, are hydrophilic, and those with longer alkyl chains are hydrophobic. A number of studies examine the solubility properties [2–5], thermoresponsive behavior [3, 6–8], aggregation [9], crystallization in solution [3, 10] and in bulk [4, 11, 12], as well as non-fouling properties [13], biocompatibility [9, 14, 15], and degradation [16] of polypeptoids.

Particularly interesting, for instance as smart drug carrier systems, are block copolypeptoids (or block copolymers in general) [17, 18] with a thermoresponsive block and a permanently hydrophilic block, which upon a change in temperature turn amphiphilic and can self-assemble into discrete aggregates, e.g., micelles or vesicles. We earlier introduced poly(*N*-(*n*-propyl)glycine)-*block*-poly(*N*-methyl glycine)s, which upon heating assemble into aggregates with a poly(*N*-(*n*-propyl)glycine) core and poly(*N*-methyl glycine) corona and continue to crystallize into very large anisotropic particles [10]. However, during the heating process, prior to crystallization, turbidimetric measurements revealed that the sample solutions did not show just a single cloud point, as could be expected, but two cloud points and a clearing point in between. Such a behavior might indicate a complex multistep assembly process, as has earlier been reported for thermoresponsive-hydrophilic poly(2-propyl-2-oxazoline)-poly(2-ethyl-2-oxazoline) block copolymers [19]. For the poly(2-oxazoline) sample, the aggregates formed at the first cloud point were found to restructure and fragment into smaller micelles, causing a clearing of the solution, and further increasing of the temperature resulted in the dehydration of both blocks and formation of large compact aggregates, causing the second cloud point.

Here, we examine the multistep aqueous solution behavior of block copolypeptoids with a long thermoresponsive poly(*N*-(*n*-propyl)glycine) block (70 units) and relatively short or evenly long hydrophilic poly(*N*-methyl glycine) block (23, 42, or 76 units), prior to the crystallization of the

✉ Helmut Schlaad
schlaad@uni-potsdam.de

[1] Department of Colloid Chemistry, Max Planck Institute of Colloids and Interfaces, Research Campus Golm, 14424 Potsdam, Germany

[2] Institute of Chemistry, University of Potsdam, Karl-Liebknecht-Straße 24-25, 14476 Potsdam, Germany

poly(*N*-(*n*-propyl)glycine) block. Phototurbidimetry and dynamic light scattering (DLS) were used to track the thermoresponsive behavior, time-dependent DLS to examine the kinetics of the association process, and transmission electron microscopy (TEM) to elucidate the structural features of the associates.

Experimental section

Polymers

A series of three poly(*N*-(*n*-propyl)glycine)$_x$-*block*-poly(*N*-methylglycine)$_y$ (P_xM_y) (subscripts indicate the degree of polymerization of the block) were synthesized by sequential nucleophilic ring opening polymerization of the corresponding *N*-alkyl glycine *N*-carboxyanhydrides, as described earlier [10]. The molecular characteristics of the block copolypeptoid samples are summarized in Table 1.

Sample preparation

Copolypeptoids were dissolved in the smallest possible volume of methanol and dried in air atmosphere overnight (to erase any crystalline domains in the samples [10]), followed by dissolution in chilled Millipore water at a concentration of 0.1 wt%. Stock solutions were stored at ~4 °C. Annealed samples were prepared by inserting the appropriate amount of stock solution into a septum-sealed vial and heating to 40 °C. Then, solutions were cooled down and used as stock solutions for following analyses.

Analytical instrumentation and methods

Turbidity measurements were performed on a turbidimetric photometer TP1 (Tepper Analytik, Wiesbaden, Germany) operating at λ = 670 nm. Samples were stirred during the heating/cooling cycles between 15 to 60 °C; heating/cooling rate was 0.1 or 1 K/min.

DLS measurements were carried out on an ALV/CGS-3 instrument equipped with a 34-mW He-Ne laser operating at $\lambda = 632.8$ nm, scattering angle $\theta = 90°$, or a Nano Zetasizer ZS (Malvern) equipped with backscatter optics. Temperature-dependent experiments were performed between 15 and 60 °C; temperature program: heating by 2.0 °C and equilibration/measurement (3 measurements at constant temperature) within 3 min; $T \pm 0.05$ °C. The raw DLS data, obtained as normalized autocorrelation functions $g_2(t)$, were analyzed using the GENDIST software, which employs the REPES algorithm to perform the inverse Laplace transformation [20]. All DLS data were taken as intensity-weighted distribution functions, while distributions diagrams are displayed in the equal area representation, $R_hG(R_h)$ [21, 22].

Analytical ultracentrifugation (AUC) measurements were carried out using an Optima XL-I analytical ultracentrifuge equipped with a Rayleigh interference optics. A 4-hole titanium rotor was operated at 25 °C and 60 K rpm. The samples were filled in 12-mm double sector center pieces made from titanium (Nanolytics, Potsdam, Germany). Sedimentation coefficient distributions were evaluated using the SEDFIT software package [23].

TEM was performed with a JEM 1011 (JEOL), operating at acceleration voltage of 80 kV. The 0.1 wt% aqueous solutions were dropped on carbon-coated copper grids and examined in the microscope after air-drying.

Table 1 Molecular characteristics of poly(*N*-(*n*-propyl)glycine)$_x$-*block*-poly(*N*-methylglycine)$_y$ (P_xM_y) copolypeptoids used in the present study (data taken from [10])

Sample	f [a]	x [b]	y [c]	M_n (kg mol^{-1}) [d]	$(M_w/M_n)^{app}$ [e]
$P_{70}M_{23}$	0.33	70	23	8.7	1.12
$P_{70}M_{42}$	0.60	70	42	10.1	1.14
$P_{70}M_{76}$	1.09	70	76	12.5	1.17

[a] Hydrophilic (M)-to-hydrophobic (P) ratio, $f = y/x$.

[b] Degree of polymerization of the poly(*N*-(*n*-propyl)glycine) (P) block.

[c] Degree of polymerization of the poly(*N*-methylglycine) (M) block.

[d] Number-average molar mass.

[e] Apparent dispersity index

Results and discussion

The turbidity heating curves for the three block copolypeptoids $P_{70}M_{23}$, $P_{70}M_{42}$, and $P_{70}M_{76}$ at 0.1 wt% (this work) and, for comparison, at 1.0 wt% ([10]) in water are shown in Fig. 1a–b. Three distinct regions, i.e., a first clouding region, followed by a period of clearing and a second clouding region, are visible on the curves for $P_{70}M_{23}$ and $P_{70}M_{42}$ and $P_{70}M_{76}$, although for the latter sample at 0.1 wt% only one transition (directly into region 3, see below) could be observed. At the first cloud point temperature, $T_{cp}^{(1)}$~27–36 °C, the P_{70} block segment collapses, and the polymer chains self-assemble into aggregates, driven by hydrophobic interactions. At the second cloud point temperature, $T_{cp}^{(2)}$~45 °C, the polymer-rich P_{70} phase of the aggregates starts to crystallize to produce large aggregate particles through a crystallization-assisted self-assembly process (see also [3, 10]). The second region, i.e., intermediate period of clearing (clearing point temperature, T_{cl}~40 °C), is not yet understood and shall here be examined in more detail.

The turbidimetric heating/cooling curves for the 0.1 wt% aqueous solutions of $P_{70}M_{23}$, $P_{70}M_{42}$, and $P_{70}M_{76}$ at different heating/cooling rates, i.e., 0.1 and 1.0 K/min, are shown in

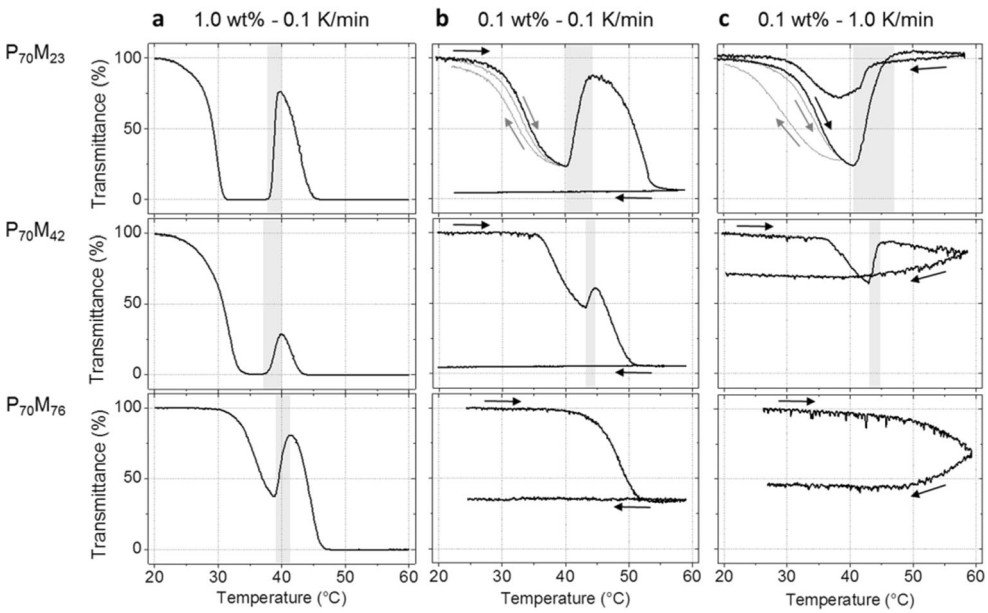

Fig. 1 Turbidimetric heating/cooling curves of aqueous solutions of block copolypeptoids $P_{70}M_{23}$, $P_{70}M_{42}$, and $P_{70}M_{76}$ at concentrations of 1.0 wt% (**a**) (data taken from [10]) and 0.1 wt% (**b**, **c**) (this work), heating/cooling rate: 0.1 (**a**, **b**) or 1.0 K/min (**c**). *Gray areas* indicate the clearing region 2

Fig. 1b–c. At the slower heating rate, the samples were allowed to reach the third region at a higher temperature and started to crystallize. Beyond this point, the process became irreversible and dispersions remained cloudy even after cooling back to room temperature (Fig. 1b), as expected from our previous work [10]. However, when the sample $P_{70}M_{23}$ was heated to <40 °C at 0.1 or 1.0 K/min, the heating/cooling cycles were reversible with hysteresis (Fig. 1b–c, gray lines). On the other hand, when the solutions of $P_{70}M_{23}$ and $P_{70}M_{42}$ were thermally treated at the faster heating/cooling rate of 1.0 K/min (Fig. 1c), the first two regions were passed, but the third region, i.e., second clouding region, was not reached even at the highest temperature of ~60 °C. Upon cooling, the process could not, or just partially, be reversed. For sample $P_{70}M_{76}$, the clouding region could not be completed until 60 °C, but nonetheless the process was irreversible upon cooling. These behaviors suggest that the association processes at a higher temperature occur under kinetic control.

In order to study the aggregation states of polymer chains from the beginning through the first clouding period to the clearance period, light scattering experiments were performed for 0.1 wt% polymer solutions in the temperature range from ~20 to 60 °C with an average heating rate of 0.6 K/min (Fig. 2). (Note: the heating of samples in light scattering experiments was faster and followed a temperature step profile, see Experimental section, which was different to the linear temperature profile in turbidimetric measurements.) Scattering intensity data indicated first and second clouding points (onset of increasing light scattering intensity) and a clearing point (onset of decreasing scattering intensity) (Fig. 2a); $T_{cp}^{(1)}$, T_{cl}, and $T_{cp}^{(2)}$ values are summarized in Table 2. Interestingly, light scattering revealed a clearing point for all three samples (T_{cl}~42–43 °C), whereas turbidity measurements showed clearing points for $P_{70}M_{23}$ and $P_{70}M_{42}$ but not for $P_{70}M_{76}$. The difference might be attributed to the different sensitivity of the two methods (measurements of scattered light vs. transmission of light).

The transitions could also be recognized by the evolution of hydrodynamic radii (R_h) with temperature, see the 2D plots for samples $P_{70}M_{23}$, $P_{70}M_{42}$, and $P_{70}M_{76}$ in Fig. 2b. The cloud point temperature ($T_{cp}^{(1)}$) for each polymer sample could be deduced from the inflection point when the hydrodynamic radii start to increase, or, more visibly, when the distribution function becomes narrow (as indicated by a more intensive color in Fig. 2b). Below $T_{cp}^{(1)}$, however, some polymer aggregates with R_h~100 nm could be observed (see below). The distributions functions reveal that the aggregates exhibit a high polydispersity (broad distribution), and polydispersity increases in the row $P_{70}M_{23} < P_{70}M_{42} < P_{70}M_{76}$ as $0.42 < 0.61 < 0.73$ (±0.01) (polydispersity values were taken as standard deviation from fitting experimental distributions by log-normal distribution function). Moreover, an additional mode could be detected for samples $P_{70}M_{42}$ and $P_{70}M_{76}$ (Fig. 2c), which exhibits a low intensity and corresponds to species with a size of 2–3 nm, i.e., molecularly dissolved polymer chains. However, it should be considered that the amount of polymer aggregates in solution could be largely overestimated by light scattering experiments (scattering intensity $\propto R^6$). In fact, AUC (data not shown) revealed just one slowly sedimenting species, suggesting that the predominant fraction in solution should be single polymer chains and not aggregates (or aggregates in just marginal amounts), as could be expected for dilute aqueous solutions of double-hydrophilic block copolymers (see also [24]).

Above $T_{cp}^{(1)}$, aggregates were formed which were remaining about constant in size, while the polydispersity values were decreasing. The following values for hydrodynamic radii and standard deviations (in brackets) at 40 °C were obtained:

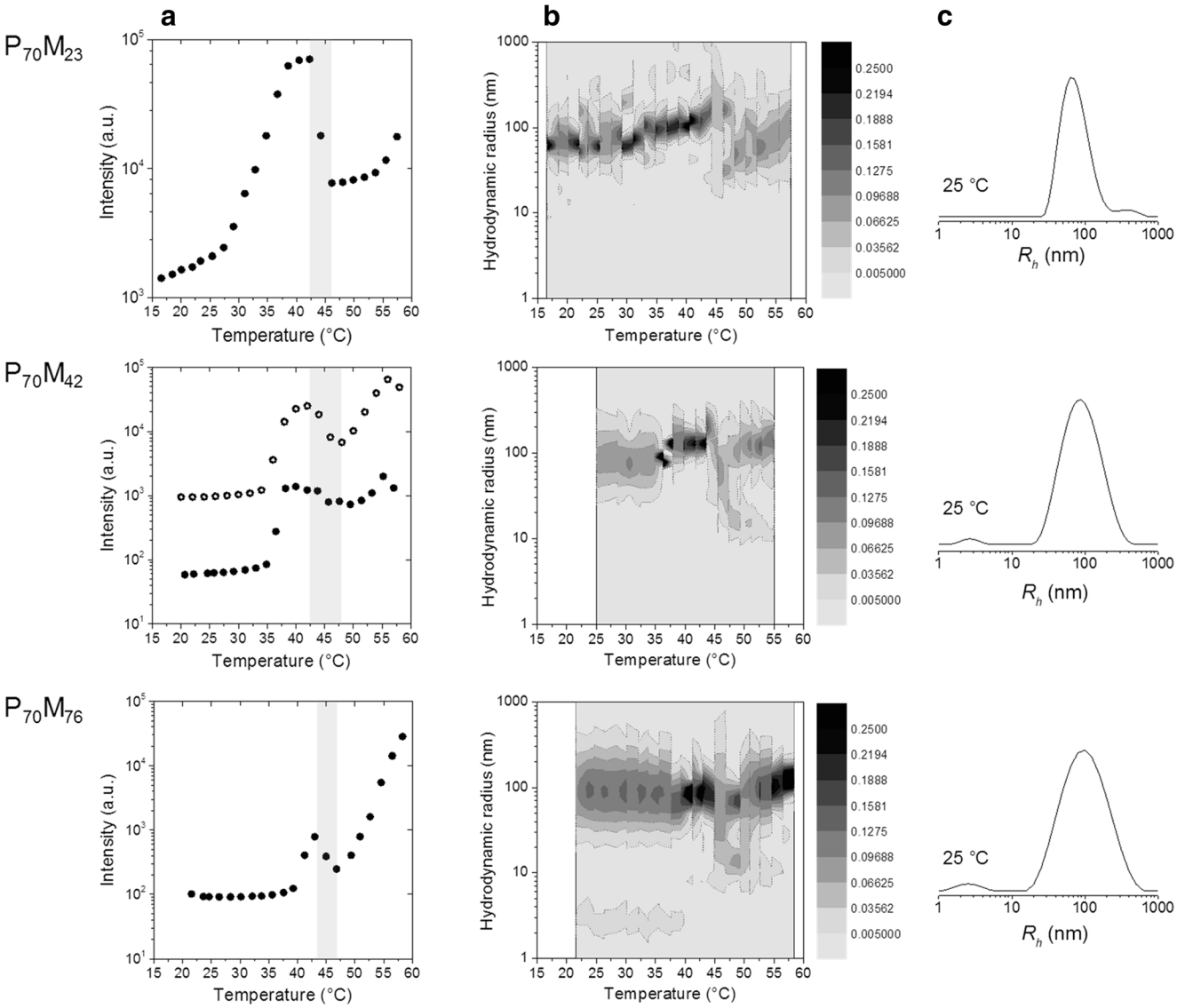

Fig. 2 Light scattering intensity data (*solid circles*, $\theta = 90°$; *open circles*, backscatter optics) (*gray areas* indicate the clearing region 2) (**a**) and 2D plots of distributions of hydrodynamic radii (R_h, $\theta = 90°$) vs. temperature (**b**) of 0.1 wt% aqueous solutions of block copolypeptoids $P_{70}M_{23}$, $P_{70}M_{42}$, and $P_{70}M_{76}$ at an average heating rate of 0.6 K/min; distributions of R_h at 25 °C (**c**)

$P_{70}M_{23}$ R_h = 103 nm (0.13), $P_{70}M_{42}$ R_h = 128 nm (0.25), and $P_{70}M_{76}$ R_h = 75 nm (0.49). When a temperature of 43–45 °C was reached, i.e., the temperature region of clearing, the system properties were changing abruptly: the radii distributions became wider and two fractions of aggregates with R_h = 15–25 nm and 80–125 nm appeared. Upon further increase of temperature, the signal from the smaller species diminished and that of the larger species became dominant (above 55 °C).

Both turbidity and light scattering measurements suggest that the thermo-induced self-assembly in the aqueous polymer

Table 2 First and second clouding and clearing point temperatures ($T_{cp}^{(1)}$, $T_{cp}^{(2)}$, and T_{cl}, respectively) of 0.1 wt% aqueous solutions of poly(*N*-(*n*-propyl)glycine)$_x$-*block*-poly(*N*-methylglycine)$_y$ (P_xM_y) copolypeptoids, as determined by turbidity and light scattering measurements

Sample	$T_{cp}^{(1)}$ (°C)		T_{cl} (°C)		$T_{cp}^{(2)}$ (°C)	
	Turbidity	Light scattering	Turbidity	Light scattering	Turbidity	Light scattering
$P_{70}M_{23}$	27	27	40	42	45	46
$P_{70}M_{42}$	36	35	43	42	45	48
$P_{70}M_{76}$	–	39	–	43	42	47

solutions follows to a certain path of transformations. Single chains at a low temperature assemble into larger aggregates above the transition temperature $T_{cp}^{(1)}$, and after reaching the temperature T_{cl}, these aggregates disassemble into smaller micelles. These micelles then grow into very large aggregates through a kinetic process, i.e., crystallization, as reported earlier [10]. Hence, the period of clearance in turbidity measurements can be ascribed to the disassembly of large aggregates (R_h > 100 nm) into small micelles (R_h = 15 or 25 nm), as has also been proposed for poly(2-oxazoline)-based block copolymers [19].

In order to trace the formation of micelles from larger aggregates, the polymer solutions were analyzed by kinetic light scattering experiments. Isothermal time-dependent measurements at $T_{cp}^{(1)} < T < T_{cl}$ (region 1) and at $T_{cl} < T < T_{cp}^{(2)}$ (region 2) were conducted for a period of 230 min; results are shown in Fig. 3a–b, respectively. (Note: measurements were examined for possible multiple scattering, which, however, seemed to have no significant impact on the evaluation of hydrodynamic radii.)

The measurements at $T_{cp}^{(1)} < T < T_{cl}$ revealed for all three polymer samples two different types of species (Fig. 3a). The first species with a size of R_h = 105–130 nm appeared at every single measurement and corresponds to the main aggregate species in solution. The second species with a size of R_h = 10–30 nm can be attributed to micelles or micelle-like structures (contour length of polymer chain (all-*trans*): 33 nm ($P_{70}M_{23}$), 40 nm ($P_{70}M_{42}$), and 50 nm ($P_{70}M_{76}$)). For the most hydrophilic $P_{70}M_{76}$, an additional third species with a size of ~3 nm could be observed, which can be attributed to single polymer chains. Also for $P_{70}M_{76}$, the two smaller species could only be detected within the first ~80 min of measurement. However, no significant changes in aggregate sizes were observed over time. The scattering intensity for $P_{70}M_{23}$ was almost constant over time whereas it increased strongly for $P_{70}M_{42}$ and $P_{70}M_{76}$. Such an increase of scattering intensity could be due to a change in aggregate size, molar mass, refractive index increment, and/or second virial coefficient. Since, no significant changes were observed in aggregate size, one can attribute the increase in intensity with an increase in molar mass (aggregation number) and/or scattering density (apart from a change in second virial coefficient upon reorganization of the aggregate surface) due to progressive dehydration and densification of the P_{70} core of aggregates [25–27]. From the intensity data, it is evident that the densification is more prominent in the row $P_{70}M_{76} > P_{70}M_{42} > P_{70}M_{23}$, i.e., decreasing hydrophilicity of polymer chains.

At $T_{cl} < T < T_{cp}^{(2)}$ (Fig. 3b), initially two species could be observed for $P_{70}M_{23}$ (R_h ~ 160 nm and ~30 nm) and $P_{70}M_{42}$ (150 nm

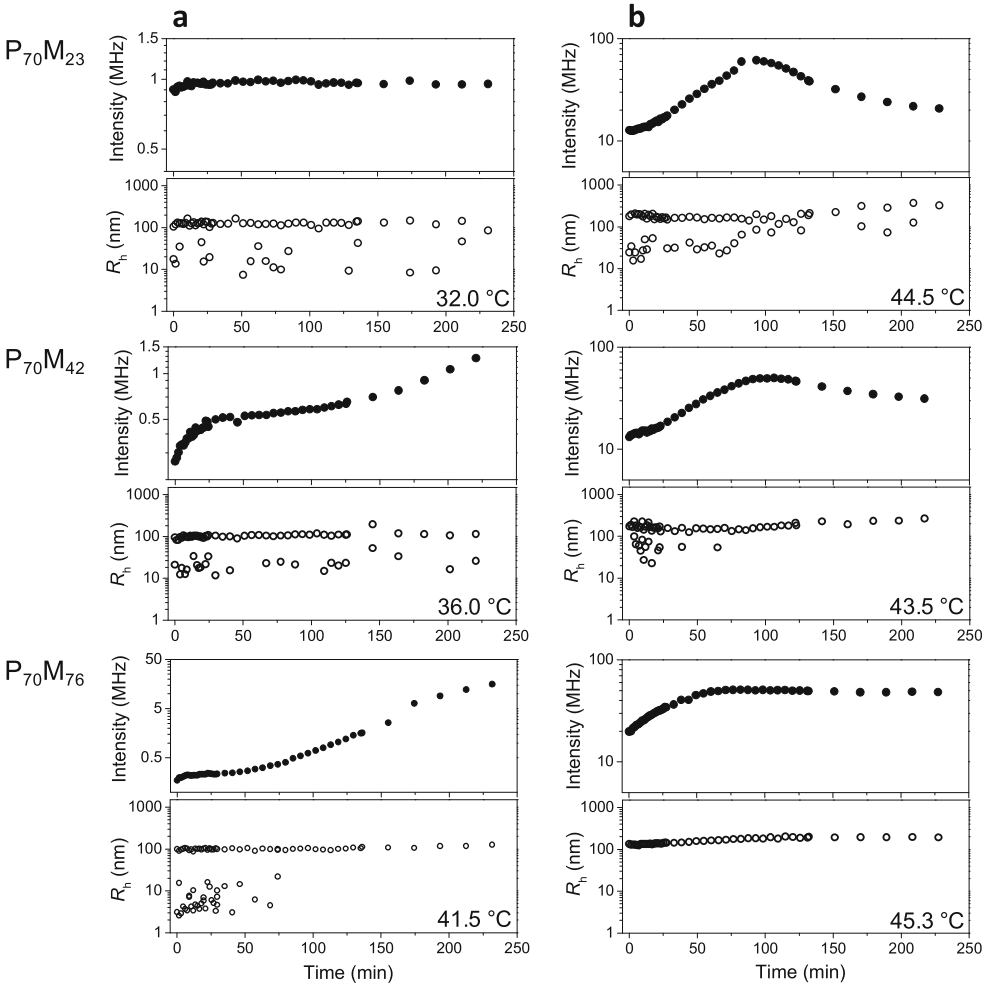

Fig. 3 Time-dependent evolution of scattering intensities and hydrodynamic radii (R_h, θ = 90°) of 0.1 wt% aqueous solutions of block copolypeptoids $P_{70}M_{23}$, $P_{70}M_{42}$, and $P_{70}M_{76}$ at $T_{cp}^{(1)} < T < T_{cl}$ (**a**) and at $T_{cl} < T < T_{cp}^{(2)}$ (**b**)

and 50 nm) and just one species for $P_{70}M_{76}$ (130 nm). Unlike before, the larger aggregates were growing in size, to R_h ~ 350 nm ($P_{70}M_{23}$), 250 nm ($P_{70}M_{42}$), and 200 nm ($P_{70}M_{76}$), with an increasing time, and the smaller aggregates disappeared within less than 100 min. The scattering intensities for $P_{70}M_{23}$ and $P_{70}M_{42}$ were also increasing with time and reached a maximum at ~100 min, coinciding with the completed transformation of the smaller aggregates into larger structures.

For a visualization of the aggregates formed at $T_{cp}^{(1)} < T < T_{cl}$, the aqueous solutions of $P_{70}M_{23}$, $P_{70}M_{42}$, and $P_{70}M_{76}$ were annealed at 40 °C for 24 h (to yield stable dispersions), dropped on a carbon-coated copper grid and analyzed by TEM after air-drying. (Note: all three samples were prepared under the same conditions which allowed for a direct comparison of, albeit collapsed, structures.) The micrographs (Fig. 4) revealed the presence of large, however, ellipsoidal particles with a length of ~350 nm and a width of ~200 nm. In the case of the most hydrophobic $P_{70}M_{23}$, the large particles are well-contrasted with a more compact inner structure surrounded by a cloud of small spherical particles. The diameter of the less contrasted spherical particles is between 15 and 40 nm, which is in the size range of micelles detected by DLS (Fig. 3a). The large particles become less contrasted in the row $P_{70}M_{23} > P_{70}M_{42} > P_{70}M_{76}$, i.e., with increasing hydrophilicity of the polymer chains (see above), indicating a less compact inner structure with a more open, sponge-like surface structure with attached micelles. In the case of $P_{70}M_{76}$, the large structures are weak aggregates with a non-compact inner structure in coexistence with smaller micelle aggregates.

The temperature-dependent aggregation behavior of the studied block copolypeptoid samples $P_{70}M_{23–76}$ in dilute aqueous solution can be summarized as follows: single polymer chains are present at low temperature, which upon heating to the first clout point temperature ($T_{cp}^{(1)}$) assemble into large aggregates ($R_h > 100$ nm) co-existing with small micelles ($R_h < 30$ nm) due to the dehydration of the P_{70} block. The large aggregates may be considered as micelle coacervates, which are well-known to be formed by non-ionic surfactants [28], or as crew-cut aggregates or large compound micelles, as described for amphiphilic diblock copolymers [29–31]. The large aggregates, however, exhibit a non-spherical (ellipsoidal) shape, and are less compact or dense the more hydrophilic are the constituting polymer chains. Upon further increasing temperature, the dehydration of polymer chains continues, thus lowering the critical micelle concentration (CMC), and segment mobility increases, ultimately resulting in the disassembly of the large aggregates into smaller micelles at the clearing point temperature (T_{cl}). The disassembly process occurred for all samples $P_{70}M_{23}$, $P_{70}M_{42}$, and $P_{70}M_{76}$, as observed by DLS, but solution clearing could only be recognized for $P_{70}M_{23}$ and $P_{70}M_{42}$, forming dense aggregates, but not for $P_{70}M_{76}$, forming just sponge-like open aggregates (TEM). At higher temperatures, the micelles start to crystallize and grow in size to produce very large crystalline particles with, again, ellipsoidal shape (see [10]).

Summary

Aqueous solutions of thermoresponsive-hydrophilic block copolypeptoids, i.e., poly(*N*-(*n*-propyl)glycine)$_x$-*block*-poly(*N*-methylglycine)$_y$ (x = 70; y = 23, 42, 76) have been investigated in the temperature range of 20–45 °C. Turbidimetric measurements indicate a multistep aggregation behavior as recognized by a sequence of a clouding region, followed by clearing period, and accomplished by second clouding region. Light scattering experiments suggest that at the first cloud point temperature single polymer chains collapse, due to dehydration of the thermoresponsive block, and assemble into large aggregates (coacervates) co-existing with small micelles. Upon further heating and reaching the clearing point temperature, the large aggregates disassemble into small micelles. When heating to the second cloud point, the micelles start to crystallize and grow in size to very large crystalline particles.

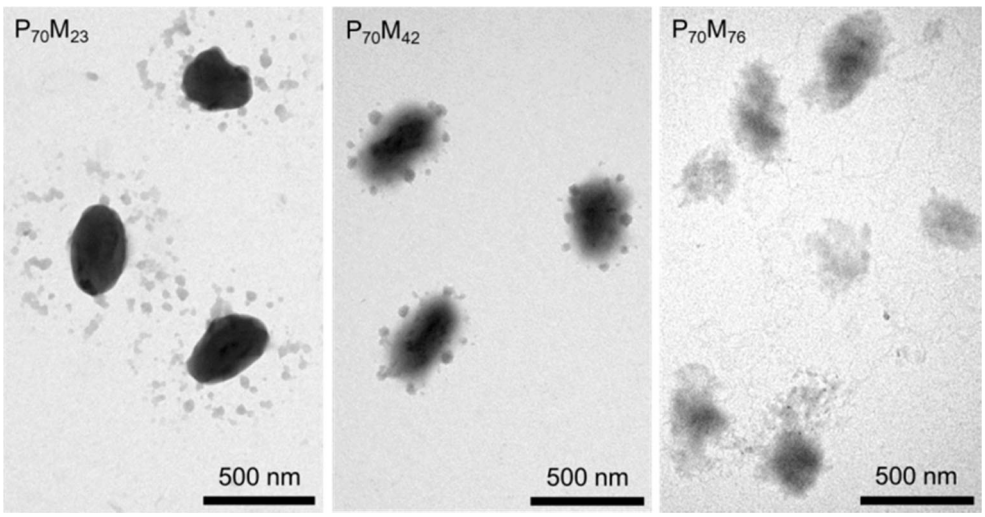

Fig. 4 Transmission electron micrographs of dried aqueous solutions of $P_{70}M_{23}$, $P_{70}M_{42}$, and $P_{70}M_{76}$ (*left to right*) after annealing at 40 °C for 24 h

Future work may be devoted to a more detailed analysis of the assembly/disassembly process of the large coacervate micelles (or crew-cut aggregates) by nuclear magnetic or electron spin electron spectroscopy and micro differential scanning calorimetry, and the analysis of their inner morphology by cryogenic transmission electron microscopy.

Acknowledgements Antje Völkel (AUC), Sibylle Rüstig (TEM), and Sascha Prentzel are thanked for their contributions to this work. Financial support was given by the Max Planck Society and the University of Potsdam.

Compliance with ethical standards

Conflict of interest The authors declare that they have no conflict of interest.

References

1. Gangloff N, Ulbricht J, Lorson T, Schlaad H, Luxenhofer R (2016) Peptoids and polypeptoids at the frontier of supra- and macromolecular engineering. Chem Rev 116:1753–1802
2. Fetsch C, Grossmann A, Holz L, Nawroth JF, Luxenhofer R (2011) Polypeptoids from N-substituted glycine N-carboxyanhydrides: hydrophilic, hydrophobic, and amphiphilic polymers with poisson distribution. Macromolecules 44:6746–6758
3. Robinson JW, Secker C, Weidner S, Schlaad H (2013) Thermoresponsive poly(N-C3 glycine)s. Macromolecules 46: 580–587
4. Guo L, Zhang DH (2009) Cyclic poly(alpha-peptoid)s and their block copolymers from N-heterocyclic carbene-mediated ring-opening polymerizations of N-substituted N-Carboxylanhydrides. J Am Chem Soc 131:18072–18074
5. Lee CU, Smart TP, Guo L, Epps TH, Zhang DH (2011) Synthesis and characterization of amphiphilic cyclic diblock copolypeptoids from N-heterocyclic carbene-mediated zwitterionic polymerization of N-substituted N-carboxyanhydride. Macromolecules 44:9574–9585
6. Lahasky SH, Hu X, Zhang D (2012) Thermoresponsive poly(α-peptoid)s: tuning the cloud point temperatures by composition and architecture. ACS Macro Lett 1:580–584
7. Lee C-U, Lu L, Chen J, Garno JC, Zhang D (2013) Crystallization-driven thermoreversible gelation of coil-crystalline cyclic and linear diblock copolypeptoids. ACS Macro Lett 2:436–440
8. Tao X, Du J, Wang Y, Ling J (2015) Polypeptoids with tunable cloud point temperatures synthesized from N-substituted glycine N-thiocarboxyanhydrides. Polym Chem 6:3164–3174
9. Fetsch C, Flecks S, Gieseler D, Marschelke C, Ulbricht J, van Pée K-H, Luxenhofer R (2015) Self-assembly of amphiphilic block copolypeptoids with C 2-C 5 side chains in aqueous solution. Macromol Chem Phys 216:547–560
10. Secker C, Völkel A, Tiersch B, Koetz J, Schlaad H (2016) Thermo-induced aggregation and crystallization of block copolypeptoids in water. Macromolecules 49:979–985
11. Lee C-U, Li A, Ghale K, Zhang D (2013) Crystallization and melting behaviors of cyclic and linear polypeptoids with alkyl side chains. Macromolecules 46:8213–8223
12. Fetsch C, Luxenhofer R (2013) Thermal properties of aliphatic polypeptoids. Polymers 5:112–127
13. Lau KHA, Ren C, Sileika TS, Park SH, Szleifer I, Messersmith PB (2012) Surface-grafted Polysarcosine as a peptoid antifouling polymer brush. Langmuir 28:16099–16107
14. Maurer PH, Subrahmanyam D, Katchalski E, Blout ER (1959) Antigenicity of polypeptides (poly alpha amino acids). J Immunol 83:193–197
15. Tanisaka H, Kizaka-Kondoh S, Makino A, Tanaka S, Hiraoka M, Kimura S (2008) Near-infrared fluorescent labeled Peptosome for application to cancer imaging. Bioconjug Chem 19:109–117
16. Ulbricht J, Jordan R, Luxenhofer R (2014) On the biodegradability of polyethylene glycol, polypeptoids and poly(2-oxazoline)s. Biomaterials 35:4848–4861
17. Dimitrov I, Trzebicka B, Müller AHE, Dworak A, Tsvetanov CB (2007) Thermosensitive water-soluble copolymers with doubly responsive reversibly interacting entities. Prog Polym Sci 32:1275–1343
18. Hoogenboom R, Schlaad H (2017) Thermoresponsive poly(2-oxazoline)s, polypeptoids, and polypeptides. Polym Chem 8:24–40
19. Trinh LTT, Lambermont-Thijs HML, Schubert US, Hoogenboom R, Kjoniksen AL (2012) Thermoresponsive poly(2-oxazoline) block copolymers exhibiting two cloud points: complex multistep assembly behavior. Macromolecules 45:4337–4345
20. Jakes J (1988) Testing of the constrained regularization method of inverting Laplace transform on simulated very wide quasieleastic light-scattering auto-correlation functions. Czechoslov J Phys 38: 1305–1316
21. Stepanek P (1993) Dynamic light scattering: the method and some applications. Clarendon Press, Oxford
22. Stepanek P, Johnsen RM (1995) Dynamic light scattering from polymer solutions: the subtraction technique. Collect Czechoslov Chem Commun 60:1941–1949
23. Schuck P (2000) Size-distribution analysis of macromolecules by sedimentation velocity ultracentrifugation and Lamm equation modeling. Biophys J 78:1606–1619
24. Casse O, Shkilnyy A, Linders J, Mayer C, Häussinger D, Völkel A, Thünemann AF, Dimova R, Cölfen H, Meier W, Schlaad H, Taubert A (2012) Solution behavior of double-hydrophilic block copolymers in dilute aqueous solution. Macromolecules 45:4772–4777
25. Garanger E, MacEwan SR, Sandre O, Brulet A, Bataille L, Chilkoti A, Lecommandoux S (2015) Structural evolution of a stimulus-responsive diblock polypeptide micelle by temperature tunable compaction of its core. Macromolecules 48: 6617–6627
26. Wanka G, Hoffmann H, Ulbricht W (1990) The aggregation behavior of poly-(oxyethylene)-poly-(oxypropylene)-poly-(oxyethylene)-block-copolymers in aqueous solution. Colloid Polym Sci 268:101–117
27. Attwood D, Collett JH, Tait CJ (1985) The micellar properties of the poly(oxyethylene) poly(oxypropylene) copolymer Pluronic-F127 in water and electrolyte solution. Int J Pharm 26:25–33
28. Kosswig K, Stache H (1993) Die Tenside. Carl Hanser Verlag, München Wien
29. Zhang LF, Eisenberg A (1995) Multiple morphologies of "crew-cut" aggregates of polystyrene-b-poly(acrylic acid) block copolymers. Science 268:1728–1731
30. Zhang L, Eisenberg A (1996) Multiple morphologies and characteristics of "crew-cut" micelle-like aggregates of polystyrene-b-poly(acrylic acid) diblock copolymers in aqueous solutions. J Am Chem Soc 118:3168–3181
31. Yu Y, Zhang L, Eisenberg A (1998) Morphogenic effect of solvent on crew-cut aggregates of amphiphilic diblock copolymers. Macromolecules 31:1144–1154

Anna Bogomolova received her B.Sc. and M.Sc. in Polymer Chemistry from Saint-Petersburg State University, Russia. She completed her Ph.D. in Physical Chemistry in 2015 at the Institute of Macromolecular Chemistry, Prague. In 2016, she joined the Max Planck Institute of Colloids and Interfaces in Potsdam for a 1-year post-doctoral fellowship under the supervision of Helmut Schlaad.

Christian Secker received his B.Sc. in Biomimetics from the University of Applied Science Bremen while conducting research on biopolymers at the Fraunhofer Institute for Manufacturing Technology and Advanced Materials (IFAM) and the MacDiarmid Research Centre, New Zealand. He received his M.Sc. in Polymer Chemistry from the Free University of Berlin in 2012 and pursued his doctoral degree under the supervision of Helmut Schlaad at the Max Planck Institute of Colloids and Interfaces. He received his Ph.D. in 2015 from the University of Potsdam and has been working since then as a senior R&D scientist at Orafol Europe GmbH in Oranienburg.

Joachim Koetz studied Chemistry at the Martin-Luther University Halle/Wittenberg and obtained his Ph.D. in Polymer Chemistry under the supervision of Burkart Philipp in 1986 from the Institute of Polymer Chemistry of the Academy of Science in Teltow-Seehof (Germany). After a post-doctoral fellowship with Esen Bekturov at the Academy of Science of Kazakhstan in Almaty, he finished his Dr.sc.nat. in 1990 and completed his habilitation at the University of Potsdam in 1992. Since 1994, he has been a professor of Colloid Chemistry at the University of Potsdam. His main interests are polyelectrolytes, liquid crystalline systems, and microemulsions as template phases for nanoparticle formation.

Helmut Schlaad studied Chemistry at the University of Mainz (Germany) and earned a doctoral degree in Physical Chemistry, under Axel H. E. Müller, in 1997. After a 1-year post-doctoral fellowship with Rudolf Faust at the University of Massachusetts in Lowell (USA), he moved to the Max Planck Institute of Colloids and Interfaces in Potsdam (Germany). He finished his habilitation in 2004, mentored by Markus Antonietti, and became a professor in 2014 at the University of Potsdam. His research interests are directed towards polymer synthesis, bio-sourced polymers, smart functional materials, and bio-inspired polymer structures.